

# Electron energy deposition in an e-beam pumped KrF amplifier: impact of the gas composition.

J. L. Giuliani

*Plasma Physics Division, Naval Research Laboratory, Washington, DC 20375*

G. M. Petrov

*Berkeley Scholars, Inc., P.O.Box 852, Springfield, VA 22150*

and A. Dasgupta

*Plasma Physics Division, Naval Research Laboratory, Washington, DC 20375*

(December 23, 2002)

## Abstract

Calculations for electron deposition in electron beam generated KrF laser at atmospheric pressure have been performed. The impact of the Ar/Kr/F<sub>2</sub> gas mixture on the electron energy distribution function, electron density and mean energy, energy per electron-ion pair, attachment, dissociation, excitation, and ionization rates have been investigated. The F<sub>2</sub> abundance controls the low energy ( $\lesssim 9$  eV) component of the distribution function, while both the fluorine and krypton mole fraction affect the distribution in the mid energy domain (9 to  $\sim 25$  eV). Consequently, the F<sub>2</sub> attachment rate coefficient varies with the F<sub>2</sub> mole fraction ( $x_{F_2}$ ) such that the electron density scales as  $1/x_{F_2}^{0.7}$ . The rate coefficient for direct dissociation of F<sub>2</sub> is smaller than for attachment but the former contributes more to the total power dissipation ( $\sim 8\%$  at  $x_{F_2} = 0.01$ ). The excitation-to-ionization ratio for Kr is not con-

Report Documentation Page				Form Approved OMB No. 0704-0188	
Public reporting burden for the collection of information is estimated to average 1 hour per response, including the time for reviewing instructions, searching existing data sources, gathering and maintaining the data needed, and completing and reviewing the collection of information. Send comments regarding this burden estimate or any other aspect of this collection of information, including suggestions for reducing this burden, to Washington Headquarters Services, Directorate for Information Operations and Reports, 1215 Jefferson Davis Highway, Suite 1204, Arlington VA 22202-4302. Respondents should be aware that notwithstanding any other provision of law, no person shall be subject to a penalty for failing to comply with a collection of information if it does not display a currently valid OMB control number.					
1. REPORT DATE <b>23 DEC 2002</b>		2. REPORT TYPE		3. DATES COVERED <b>00-00-2002 to 00-00-2002</b>	
4. TITLE AND SUBTITLE <b>Electron energy desposition in an e-beam pumped KrF amplifier: impact of the gas composition</b>				5a. CONTRACT NUMBER	
				5b. GRANT NUMBER	
				5c. PROGRAM ELEMENT NUMBER	
6. AUTHOR(S)				5d. PROJECT NUMBER	
				5e. TASK NUMBER	
				5f. WORK UNIT NUMBER	
7. PERFORMING ORGANIZATION NAME(S) AND ADDRESS(ES) <b>Naval Research Laboratory, Plasma Physics Division, Code 6730, Washington, DC, 20375</b>				8. PERFORMING ORGANIZATION REPORT NUMBER	
9. SPONSORING/MONITORING AGENCY NAME(S) AND ADDRESS(ES)				10. SPONSOR/MONITOR'S ACRONYM(S)	
				11. SPONSOR/MONITOR'S REPORT NUMBER(S)	
12. DISTRIBUTION/AVAILABILITY STATEMENT <b>Approved for public release; distribution unlimited</b>					
13. SUPPLEMENTARY NOTES					
14. ABSTRACT <b>see report</b>					
15. SUBJECT TERMS					
16. SECURITY CLASSIFICATION OF:			17. LIMITATION OF ABSTRACT <b>Same as Report (SAR)</b>	18. NUMBER OF PAGES <b>27</b>	19a. NAME OF RESPONSIBLE PERSON
a. REPORT <b>unclassified</b>	b. ABSTRACT <b>unclassified</b>	c. THIS PAGE <b>unclassified</b>			

stant, as generally assumed, but increases by a factor of two with a decrease in either the Kr or F<sub>2</sub> abundance. Combining the former and present investigations leads to a set of fitting formulas to be used in beam kinetics codes for various collision rates as a function of both the electron beam power density and the composition.

PACS: 52.40.Mj, 42.55.Lt, 52.20.Fs, 52.25.Dg

## I. INTRODUCTION

Large aperture KrF\* amplifiers at atmospheric pressure, pumped by intense electron beams, are the most promising laser systems for inertial confinement fusion energy.<sup>1-7</sup> Understanding the electron energy deposition leading to the subsequent kinetic reactions is essential for scaling models of existing amplifiers to those required for a fusion driver. In a previous article<sup>8</sup> we developed a detailed model for solving the spatially averaged, time independent electron Boltzmann equation from the beam energy down to zero kinetic energy in order to evaluate the ionization and excitation rates in a beam generated Ar-Kr-F<sub>2</sub> plasma. The electron energy distribution function (EEDF), electron mean energy and density, branching ratios for various energy channels, energy per electron-ion pair, and stopping power were investigated at different beam powers and beam energies but for a fixed composition (68.53% Ar, 31% Kr, 0.47% F<sub>2</sub>). We concluded that the EEDF is sensitive to the beam power density but not the beam energy as long as the latter is above 10 keV. At low power densities (few kW/cm<sup>3</sup>) the electron density is also low and the distribution is non-thermal since the Coulomb electron collisions are insufficient to overcome the inelastic collisions with rare gas atoms. At high power densities ( $\sim 1$  MW/cm<sup>3</sup>) the electron density is sufficient to relax the EEDF toward a Maxwellian. Based on the Boltzmann analysis the calculated excitation-to-ionization ratio for Ar was found to be  $\sim 0.4$ , which is  $\sim 25\%$  higher than the ratio found from the Continuous Slowing Down Approximation.<sup>9</sup> Furthermore, the same ratio for Kr was found to increase from 0.54 to 0.8 as the beam power increases. Both of these ratios are significantly higher than the values (0.28-0.30) used in existing kinetic models of KrF amplifiers.<sup>10-14</sup>

Now consider how variations in the fluorine and krypton mole fractions might impact the e-beam deposition, particularly the excitation processes. A change of the fluorine mole fraction alters the EEDF due to the competition between thermal relaxation of the bulk electrons and inelastic losses with fluorine involving low energy electrons, such as attachment, vibrational excitation, and impact dissociation. Furthermore, the abundance of F<sub>2</sub> controls

the density of electrons through dissociative attachment. An increase in  $F_2$  lowers the electron density and should have a similar effect upon the low energy part of the EEDF as a decrease in the beam power. For Kr, as its abundance increases over that of Ar, the energy at which the EEDF is depleted by inelastic collisions with the rare gases shifts from the first excitation potential of Ar to the corresponding lower one of Kr. This leads to a lower excitation rate for Kr. It can be surmised that excitation reactions for  $F_2$ , Kr, and Ar will be dependent upon the gas composition as well as the beam power.

The objective of the present study is to investigate the EEDF, the resultant ionization and excitation rates of Ar and Kr, and the ionization, excitation, dissociation and attachment rates to  $F_2$  molecules as a function of the gas composition in an e-beam pumped KrF amplifier. In the next section the reaction processes are examined in detail as the fluorine abundance is varied for a fixed Ar and Kr pressure, and a fixed beam power. Section III follows the same pattern but for the variation in Kr. Section IV generalizes the above particular results by presenting approximate algebraic relations for the excitation and ionization rates of Ar, Kr, and  $F_2$  as a function of both electron beam power and composition. These results provide an improved description of the electron beam deposition for use in kinetic models of KrF amplifiers.

## II. PLASMA PARAMETERS VERSUS FLUORINE MOLE FRACTION

For the results presented below the beam power density, beam energy and gas temperature are fixed at  $P_{beam}=346$  kW/cm<sup>3</sup>,  $U_{beam}=100$  keV and  $T_g=300$  K. The Ar and Kr pressures are also fixed at  $p_{Ar}=562.5$  Torr and  $p_{Kr}=254.4$  Torr. The fluorine mole fraction is varied to investigate the dependence of the EEDF, and the excitation and ionization rates on this parameter. Specifically, the fluorine mole fraction  $x_{F_2} = n_{F_2}/(n_{Ar} + n_{Kr} + n_{F_2})$  is varied from 0.1% to 3% of the total density. This composition includes the range used in KrF\* amplifiers.

The EEDF is calculated from the steady state solution of the Boltzmann equation using

a large set of cross sections for inelastic collisions with Ar, Kr, and F<sub>2</sub>, as well as electron Coulomb collisions. Details are described in Ref. 8. Results for the EEDF are presented in Fig. 1a as a function of the fluorine mole fraction in the discharge. The EEDF  $f(u)$ , where  $u$  is the electron energy, is related to the electron density through  $n_e = \int f(u) du$ . The same results, but for the normalized distribution  $\tilde{f}(u) = f(u)/(n_e u^{1/2})$ , is shown in Fig. 1b. In this case  $\int \tilde{f} u^{1/2} du$  is unity. This latter depiction is useful for the discussion concerning the electron reaction rate coefficients presented below. In the low energy region, i.e., below the excitation threshold of Kr at 9.9 eV, the EEDF  $f(u)$  is formed by elastic scattering with Ar and Kr, and more importantly, by attachment, vibrational excitation, and dissociation with F<sub>2</sub> molecules. For a negligible mole fraction of fluorine, the EEDF is Maxwellian up to a kinetic energy of  $\sim 9$  eV (straight line in a log-linear plot of  $f(u)/u^{1/2}$ ). From the first paper an increase of the beam power per unit volume for a fixed F<sub>2</sub> abundance was found to increase the degree of ionization, which in turn relaxes  $f(u)$  toward a Maxwellian EEDF. Now we see that a reduction of the fluorine mole fraction also leads to a Maxwellian distribution of the core electrons due to the increase in electron density. At a mole fraction of 1%, dissociation and excitation of F<sub>2</sub> become more important than the elastic collisions with the rare gases and the EEDF deviates from Maxwellian. Furthermore, dissociative attachment to F<sub>2</sub> molecules depletes the EEDF and decreases the total number of electrons. One can see from Fig. 1a that at the high F<sub>2</sub> fraction of 3%, the EEDF below  $\sim 2$  eV even turns downwards due to attachment. The dissociation of F<sub>2</sub>, which has a threshold of 3.16 eV and peaks at  $\sim 7$  eV, also leads to a depletion of electrons in this energy range. In the mid energy region, between the excitation and ionization thresholds of the rare gases ( $\sim 9$  to  $\sim 15$  eV), the inelastic collisions of electrons with fluorine are less important than with Ar and Kr. As the fluorine abundance increases one sees that the flux of electrons into the low energy region cannot be compensated by electron Coulomb collisions leading to relaxation. One may then expect a dependence of the Ar and Kr excitation rates on the fluorine mole fraction. In the high energy region ( $u \gtrsim 15$  eV) the EEDF is formed by ionization of the target species, Ar, Kr, and F<sub>2</sub>, and the production of secondary electrons by the energetic

beam. Due to the negligible fraction of  $F_2$  compared to both Ar and Kr, the EEDF is not affected by variation of the fluorine density. As a consequence, the total ionization rate of the target gas ( $R_{tot}^{ion}$ ) is independent of the fluorine mole fraction. One can conclude that the low energy part of the EEDF, below the ionization threshold, is very sensitive to fluorine, while the high energy part of the EEDF is not.

Fig. 2 shows the electron density  $n_e$  and mean energy of the bulk electrons  $\langle u \rangle$  versus the fluorine mole fraction. The electron density, calculated from  $n_e = R_{tot}^{ion}/(k^{att}n_{F_2})$ , is found to vary as  $1/n_{F_2}^{0.7}$ . The deviation from the simple inverse linear relation commonly assumed arises from the dependence of the attachment rate coefficient ( $k^{att}$ ) on the low energy component of the EEDF, which itself varies with the  $F_2$  mole fraction.  $\langle u \rangle$  represents the average energy of electrons with kinetic energies  $u < 30$  eV. The mean energy of these bulk electrons, related to the effective electron temperature through  $T_e = (2/3)\langle u \rangle$ , increases with the fluorine mole fraction. At 0.1% fluorine mole fraction  $\langle u \rangle$  is 2.1 eV, while for mole fractions between 1.5% and 3% it is 3 eV. This variation reflects changes of the low energy part of the EEDF resulting from electron-molecule inelastic collisions.

The individual species ionization rates,  $R_\alpha^{ion}$ , are determined from the solution of the steady state, spatially independent, electron Boltzmann equation subject to the given beam power, beam voltage, gas density and composition. In steady state the sum over all ionization rates equals the attachment rate:  $R_{tot}^{ion} = R^{att}$ . Since fluorine has no impact on  $f(u)$  above the ionization thresholds of Ar and Kr, the ionization rates of both Ar and Kr are not influenced by the fluorine. Only the ionization rate of fluorine increases due to an increase of the fluorine mole fraction, though even at the highest mole fraction considered (3%), it is less than 1% of the combined Ar and Kr ionization rates.

The strong variation of the EEDF and  $n_e$  with the fluorine mole fraction impacts the reaction *rate coefficients* as shown in Fig. 3. The ionization rate coefficient is calculated from  $k_\alpha^{ion} = R_\alpha^{ion}/(n_en_\alpha)$ , and likewise for the other processes. As the fluorine mole fraction increases from 0.1% to 3%, the corresponding rate coefficient for valence shell ionization of Ar increases from  $0.19 \times 10^{-11}$  to  $2.1 \times 10^{-11}$  cm<sup>3</sup>/s, and for inner shell ionization from

$0.46 \times 10^{-13}$  to  $5.0 \times 10^{-13}$  cm<sup>3</sup>/s. A tenfold increase of the ionization rate coefficient (both valence and inner shell) is also observed for Kr and F<sub>2</sub>. The increase of the lumped electron impact excitation rate coefficients for Ar, Kr, and F<sub>2</sub> with the fluorine mole fraction is likewise nearly a factor ten. For simplicity all excitation terms of Ar are summed together and likewise for Kr. For F<sub>2</sub> the excitations are to stable electronic states above 11 eV. On the other hand, the increase with  $x_{F_2}$  of the rate coefficient for direct dissociation,  $k^{dis}$ , is only a factor of two (Fig. 3c). Recall that the energy threshold for this process is  $\sim 3$  eV. Note that  $k^{dis}$  is almost two orders of magnitude larger than the sum of the excitation rate constants for both Ar and Kr. The vibrational excitation of fluorine has an even lower threshold and the rate coefficient decreases as the fluorine mole fraction increases. The same holds for attachment to F<sub>2</sub>, which has a zero energy threshold. Thus the general trends in the variation of the rate coefficients with the fluorine mole fraction, observed in Fig. 3, can be outlined as follows. Increase of fluorine leads to a strong increase of the rate coefficients for inelastic processes having a large energy threshold. Moderate increase of the rate coefficients occurs for processes with an energy threshold of few eV, and a decrease of the rate coefficients occurs for processes with low or no energy threshold.

The key to understanding the behavior of the rate coefficients is the normalized EEDF,  $\tilde{f}(u)$ . While the rates involve the EEDF  $f(u)$  shown in Fig. 1a, the rate coefficients are evaluated from integrals over the normalized distribution  $\tilde{f}(u)$  of Fig. 1b. For kinetic energies exceeding the ionization thresholds of Ar, Kr, and F<sub>2</sub> (14 to 15.7 eV),  $\tilde{f}(u)$  increases as the fluorine mole fraction increases, and hence so do the ionization rate coefficients. The same effect explains the increase in the rate coefficients for excitation of Ar and Kr. These latter processes are susceptible to changes of  $\tilde{f}(u)$  for kinetic energies above 9.9 eV. For kinetic energies between 2 and  $\sim 9$  eV the normalized EEDF has a complex structure. Whether a rate coefficient will increase or decrease depends on the process threshold and the energy dependence of the cross section. For example, the dissociation rate coefficient increases with the fluorine mole fraction for small  $x_{F_2}$ , passes through a maximum, and then decreases for  $x_{F_2} > 1.4\%$ . Between zero and 2 eV,  $\tilde{f}(u)$  decreases proportionally to the fluorine mole

fraction as a result of attachment. Thus rate coefficients for kinetic processes whose main contribution is in this energy region, such as attachment and vibrational excitation of  $F_2$ , decrease as the fluorine mole fraction increases.

The individual power balance terms are plotted in Fig. 4. These terms are normalized to the beam power deposition  $P_{beam}$ . As above, all the excitation processes for Ar and Kr are separately lumped. The fractional power deposition for most processes involving Ar and Kr decreases somewhat with the fluorine mole fraction. As one would expect, the power deposition in  $F_2$  increases with the fluorine mole fraction. Note from Fig. 4c that this deposition into  $F_2$  accounts for 5 to 15% of the total power loss in the target gas, significantly higher than the fractional abundance of  $F_2$ . The most important channel in the  $F_2$  deposition is direct dissociation ( $F_2 + e^- \rightarrow 2F + e^-$ ). Attachment accounts for 2 to 3%, and the contribution of each of the other power loss channels (elastic scattering, vibrational excitation, excitation to electronically excited states and ionization) is less than 1%.

These results for power deposition in e-beam pumped target gas as a function of  $x_{F_2}$  can be compared with a similar figure for the fractional power transfer in an e-beam sustained Ar-Kr- $F_2$  discharge presented by Nighan.<sup>15</sup> In the beam sustained discharge the power input by the beam is about one-third of the total power, i.e., resistive heating of the core electrons is dominant. Nighan calculated that at  $x_{F_2} = 1\%$  the total excitation of the rare gases accounts for  $\sim 50\%$ , elastic losses are  $\sim 12\%$ , and  $F_2$  direct plus attachment dissociation is  $\sim 35\%$ . These values are significantly higher than shown in Fig. 4 for the beam pumped discharge. In this latter case ionization is the dominant power transfer channel due to the enhanced tail of the EEDF arising from the secondary electrons as the primaries slow down.

### III. PLASMA PARAMETERS VERSUS KR MOLE FRACTION

The second parameter to be examined is the Kr mole fraction. In the present section the total pressure of Ar plus Kr is fixed at 816.9 Torr and the fluorine pressure is kept at

3.9 Torr ( $x_{F_2}=0.47\%$ ). The plasma parameters are presented versus the mole fraction of Kr:  $x_{Kr} = n_{Kr}/(n_{Ar} + n_{Kr} + n_{F_2})$ . In the NIKE KrF\* amplifier Ar is the dominant gas ( $\sim 70\%$ ), but other experiments have been performed in Kr rich mixtures.<sup>16</sup> In this work  $x_{Kr}$  is varied from 10% to 90%. Results for the normalized EEDF  $\tilde{f}(u)$  in the energy region 0-25 eV are presented in Fig. 5. The EEDF depends on the Kr mole fraction only for kinetic energies between  $\sim 9$  eV and  $\sim 25$  eV, which is associated with the excitation and ionization processes of Kr. As  $x_{Kr}$  increases the EEDF becomes depleted within this energy region due to the lower excitation threshold and the larger ionization cross section of Kr compared to Ar (see Figs.2 and 4 of Ref. 8). For energies below  $\sim 9$  eV the Kr mole fraction does not affect the EEDF, and consequently, the mean electron energy changes only slightly (from 2.79 eV to 2.71 eV) as  $x_{Kr}$  increases from 10% to 90%.

The impact of the krypton mole fraction on the rate coefficients is shown in Fig. 6. The rate coefficients for electron impact excitation and ionization of Ar decrease by  $\sim 25\%$  as  $x_{Kr}$  increases. The largest variation is in the lumped rate coefficient for electron excitation of Kr, which decreases by a factor of two (Fig. 6b). This reflects the depletion of the EEDF between  $\sim 9$  and  $\sim 25$  eV as shown in Fig. 5. The excitation and ionization rate coefficients of fluorine are weakly dependent on the krypton mole fraction, while the vibrational excitation, attachment, and dissociation rate coefficients are independent of the Kr mole fraction due to their low energy thresholds.

The individual contributions to the power balance, normalized by the beam power density  $P_{beam}$ , are plotted in Fig. 7. Note that as the Kr abundance increases the power deposition into Kr excitation does not grow as fast as that into Kr ionization. This feature likewise stems from the depletion of the EEDF near  $\sim 9$  eV. The power deposition in  $F_2$  is independent of the krypton mole fraction, except for the electron impact ionization and excitation to high lying molecular electronic states. As before, the main contributions to the power deposition rate in fluorine are the electron impact dissociation, attachment to  $F_2$  molecules and vibrational excitation. All of them have low energy thresholds, in the energy region where the EEDF is independent of the Kr mole fraction.

## IV. IONIZATION AND EXCITATION RATES AS A FUNCTION OF BEAM POWER AND COMPOSITION

### A. Energy per electron-ion pair and ionization rates

In the previous sections the trends in ionization and excitation were examined for a fixed e-beam power deposition and separately for variations in the  $F_2$  and Kr mole fractions. As reviewed in the Introduction, the first paper<sup>8</sup> examined the dependence of these processes on the beam power with a fixed composition. In applications to the kinetics of a beam generated KrF amplifier it would be useful to have convenient formulas for the ionization and excitation rates as a function of both the beam power and composition. The relations presented below are based on fits to the results from a number of calculations and are valid for a fluorine mole fraction  $0.2\% < x_{F_2} < 2\%$ , any argon and krypton mole fractions, and an input power density between  $100 \text{ kW/cm}^3$  and  $1 \text{ MW/cm}^3$ .

The energy per electron-ion pair  $\mathcal{W}_{ei}$  can be approximated with a quadratic function in the Kr mole fraction

$$\mathcal{W}_{ei} = 25 - 1.49x_{Kr} + 0.45x_{Kr}^2 \text{ (eV)} . \quad (1)$$

The previous paper noted that the calculated  $\mathcal{W}_{ei}$  for pure Ar is  $\sim 4\%$  lower than some measured values, but the results for pure Kr match the data. Within the above limits, the abundance of  $F_2$  does not affect  $\mathcal{W}_{ei}$  because the ionization potential of  $F_2$  is similar to that of Ar and Kr and the predominance of the latter species control the EEDF above  $\sim 15 \text{ eV}$ . Equation (1) is used to compute the total number of ionizations per unit volume, per unit time:

$$R^{ion} = \frac{P_{beam}}{k_B \mathcal{W}_{ei}} . \quad (2)$$

Boltzmann's constant is present to convert eV to the chosen energy units in  $P_{beam}$ . The ionization rate  $R_\alpha^{ion}$  of each species  $\alpha = \text{Ar, Kr, } F_2$  is expressed as a fraction of the total ionization rate  $R^{ion} = \sum_\alpha R_\alpha^{ion}$ . For  $\alpha = \text{Ar or Kr}$  the ionization processes include valence

shell, inner shell, and Auger ionization. For  $\alpha = \text{F}_2$  only valence shell ionization is considered. We find that  $R_\alpha^{ion}$  is proportional to the species mole fraction and a function depending on the composition:

$$R_\alpha^{ion} = x_\alpha \gamma_\alpha R^{ion}. \quad (3)$$

where  $\gamma_{Ar} = 1/(x_{Ar} + 1.6x_{Kr} + 0.35x_{F_2})$ ,  $\gamma_{Kr} = 1.6\gamma_{Ar}$ , and  $\gamma_{F_2} = 0.35\gamma_{Ar}$ . The sum  $\sum_\alpha x_\alpha \gamma_\alpha$  equals unity.

### B. Excitation-to-ionization ratios

The excitation-to-ionization ratio for species  $\alpha$  is specified by

$$\eta_\alpha^{exc} = \frac{\sum_\ell R_{\alpha,\ell}^{exc}}{R_\alpha^{ion}} \quad (4)$$

For the rare gases the numerator is the sum over excitations to all levels  $\ell$  enumerated in Ref. 8 and for  $\text{F}_2$  the numerator includes excitations to the  $\text{C}^1\Sigma_u^+$  and  $\text{H}^1\Pi_u$  molecular electronic states. Results for  $\eta_\alpha^{exc}$  are displayed in Fig. 8 for a beam power density of  $346 \text{ kW/cm}^3$ . While the excitation-to-ionization ratios of Ar and  $\text{F}_2$  are weakly dependent on both the fluorine and krypton mole fractions,  $\eta_{Kr}^{exc}$  depends on both parameters. For small  $\text{F}_2$  and Kr mole fractions the excitation-to-ionization ratio of Kr approaches unity, i.e. there is approximately one excitation per ionization. In this case the formation of the EEDF is predominantly due to collisions with Ar atoms. As a result, the EEDF above the excitation threshold of Kr and below that of Ar is more populated than it is in the case of pure Kr. The decrease in the Kr excitation efficiency with an increase in either the  $\text{F}_2$  or Kr mole fractions reflects the impact of electron inelastic collisions with these species on the EEDF near 9 eV.

To account for the dependence of  $\eta_\alpha^{exc}$  on both beam power density and composition we have developed a general relation describing our calculations:

$$\eta_\alpha^{exc} = (A_\alpha + B_\alpha e^{-3.5x_{Kr}}) P_{beam}^{C_\alpha}. \quad (5)$$

Here  $A_{Ar} = 0.412/(1 + 2x_{F_2})$ ,  $B_{Ar} = 0.063e^{-90x_{F_2}}$ ,  $C_{Ar} = 0.03$ ;  $A_{Kr} = 0.744/(1 + 17x_{F_2})$ ,  $B_{Kr} = 0.555e^{-64x_{F_2}}$ ,  $C_{Kr} = 0.10$ ; and  $A_{F_2} = 0.464/(1 + 2x_{F_2})$ ,  $B_{F_2} = 0.106e^{-110x_{F_2}}$ ,  $C_{F_2} = 0.045$ .  $P_{beam}$  is in units of MW/cm<sup>3</sup>.  $\eta_{Kr}^{exc}$  is the most strongly dependent on the beam power. For instance,  $\eta_{Kr}^{exc}$  increases by about 30% as the input power increases from 0.1 to 1 MW/cm<sup>3</sup>, while for Ar the increase is only  $\sim 5\%$ . The dependence of  $\eta_{\alpha}^{exc}$  on the F<sub>2</sub> concentration arises from the influence of fluorine on the EEDF below  $\sim 15$  eV (see Fig. 1).

The results of Fig. 8 and Eq. (5) are particularly relevant to calculations of the kinetics within an electron beam pumped KrF amplifier. To date kinetic models<sup>10–14</sup> have assumed  $\eta_{Kr}^{exc}$  to be a constant independent of power or composition and have typically set its value to that for Ar as found from the Continuous Slowing Down Approximation ( $\eta_{Ar}^{exc} = 0.28$ ),<sup>9</sup> or slightly larger. The excitation-to-ionization ratio for Kr as calculated here is significantly larger than that for Ar and strongly depends on the gas composition.

### C. Rate coefficients for low energy processes with F<sub>2</sub>

The rates for F<sub>2</sub> ionization and electronic excitation to bound states are given as part of Eqs. (3) and (5). The energy thresholds for these processes are 15.7 and 11.5 eV, respectively. Other collisional processes involving F<sub>2</sub> have energy thresholds below the lowest excitation level of the rare gases. We have examined three reactions, namely attachment (threshold of 0 eV), vibrational excitation (0.11 eV), and excitation to the dissociating molecular states  $a^3\Pi_u$  (3.2 eV) and  $A^1\Pi_u$  (4.3 eV). Rate coefficients for these latter reactions have been determined from their respective cross sections<sup>17</sup> and the calculated EEDF. Fitting formulas are presented in Table I. The dependence upon the mole fraction of F<sub>2</sub> arises from the strong variation of the low energy part of the EEDF with  $x_{F_2}$  as shown in Fig. 1. Since the e-beam power deposition also affects the low energy domain of the EEDF, the power dependence is included for the rate coefficients of Table I.

The attachment rate coefficient of Table I for characteristic parameters of a KrF amplifier ( $x_{F_2} \sim 0.003$  and  $P_{beam} \sim 500$  kW/cm<sup>3</sup>) gives  $1.9 \times 10^{-9}$  cm<sup>3</sup>/s, which is in agreement with

the compilation of values by McCorkle, *et al.*<sup>18</sup> This comparison is made against their Fig.3 for an effective electron temperature between 1.4 and 2 eV based on the mean energies in our Fig. 2. The direct dissociation rate coefficient for the same parameters is  $6.4 \times 10^{-10}$  cm<sup>3</sup>/s, a factor of two larger than the value assumed in the KrF kinetics codes of Refs. 10, 14, but a factor of seven less than that proposed by Kushner and Moratz<sup>19</sup> based on the comparison of a kinetics code with electron density measurements in a beam excited Ne/Xe/F<sub>2</sub> mixture. Direct dissociation is an important process in KrF amplifiers as it is the largest contributor to the power deposition by the fluorine species and it leads to F<sub>2</sub> burn-up. We have convolved a Maxwellian distribution at  $T_e = 2$  eV with the cross section data<sup>20</sup> used by Kushner and Moratz and found  $k^{dis}$  to be closer to our estimate. Furthermore, with the cross sections used in our present Boltzmann calculations,  $k^{dis}$  for a 3 eV Maxwellian distribution is  $1.8 \times 10^{-9}$  cm<sup>3</sup>/s, which agrees with the experimental value measured at 3 eV by Elyaakoubi and Ranson.<sup>21</sup> Since  $k^{dis}$  decreases with decreasing  $T_e$ , and the effective temperatures computed for an e-beam pumped KrF amplifier are  $\sim 1.4$  to 2 eV, we believe our results for  $k^{dis}$  are consistent with the recent data.

## V. SUMMARY

The first paper in this series<sup>8</sup> examined the EEDF resulting from an e-beam deposition into an Ar-Kr-F<sub>2</sub> target gas appropriate to a KrF laser amplifier. The power deposition was varied and the ionization and excitation rates of the constituent species were calculated from the EEDF for a fixed composition. The present paper complements the former work by investigating the EEDF and the consequent inelastic rates for different gas mixtures but for a fixed power deposition.

The EEDF  $f(u)$  is used to evaluate the power deposition of various reactions through the rates such as ionization  $R^{ion}$ , attachment  $R^{att}$ , etc. Figure 1a indicates that the low energy part ( $\lesssim 9$  eV) of  $f(u)$  is sensitive to the F<sub>2</sub> mole fraction, while the high energy part above the ionization thresholds ( $\gtrsim 15$  eV) is not. Thus the ionization rates for Kr and Ar are

independent of  $x_{F_2}$  as shown in Fig. 4, while the rate coefficients for the low energy inelastic collisions with fluorine are themselves dependent on the  $F_2$  abundance. Although direct dissociation of  $F_2$  has not been included in most KrF kinetics code, it accounts for most of the power deposition through the  $F_2$  species even though its rate coefficient is smaller than that for attachment. Together direct dissociation and attachment account for  $\sim 5\%$  of the total power deposition at only  $x_{F_2} = 0.1\%$ , and rise to  $\sim 15\%$  at  $x_{F_2} = 3\%$ . Comparing the results from Fig.7 of Ref. 8 with the present analysis, we conclude that the effect on the EEDF of changing  $x_{F_2}$  is opposite to that of changing  $P_{beam}$ .

The normalized distribution  $\tilde{f}(u)$  of Fig. 1b is used to calculate the rate coefficients for inelastic processes. The variation of  $\tilde{f}(u)$  with  $x_{F_2}$  is not uniform, but rather exhibits different behavior depending on the electron energy domain. For instance, the attachment rate coefficient, which is sensitive to the low energy component of  $\tilde{f}(u)$ , varies with  $x_{F_2}$  because the latter controls the electron density which in turn effects the thermalization of the EEDF. As a result we find  $n_e \propto 1/n_{F_2}^{0.7}$  instead of an inverse linear relation.

While the ionization rate due to e-beam deposition can be evaluated from the measured energy per ion-electron pair,<sup>22</sup> the excitation-to-ionization ratio  $\eta^{exc}$  must be determined from theoretical calculations. This value is important in KrF kinetics since there are channels leading to KrF formation through excited Ar and Kr. The use of a constant rate coefficient in a KrF kinetics model for, say, Kr excitation (see Ref. 14), could not reproduce the behavior presented in Fig. 3. Even an Arrhenius form with a temperature dependence (see Ref. 13) would be inaccurate as the effective electron temperature from Fig. 2 changes only slightly above  $x_{F_2} \sim 1\%$ , unlike the calculated rate coefficient for Kr excitation as a function of  $x_{F_2}$ . Figure 8 indicates that at a fixed power the excitation-to-ionization ratio for Ar and  $F_2$  vary weakly with gas composition, but  $\eta_{Kr}^{exc}$  decreases significantly with an increase in either  $x_{F_2}$  or  $x_{Kr}$ . This arises from the depletion of electrons in the EEDF above the first excitation threshold of Kr.

Finally the results of the first paper are combined with the present analysis to develop analytic fitting formulas for the energy per electron-ion pair, ionization rates, and excitation-

to-ionization ratios as a function of both the gas composition and input power per unit volume. These formulas can be conveniently incorporated unto KrF kinetics codes to properly describe the power input by an electron beam to the internal energy of the target gas.

### **ACKNOWLEDGMENTS**

We wish to thank Robert Lehmberg, John Sethian, and Steve Obenschain of the Laser Physics Branch at NRL, Steve Swanekamp of JAYCOR, and Stu Searles of RSI for many fruitful discussions related to e-beam deposition. This work was supported by the US Department of Energy, Defense Programs.

## REFERENCES

- <sup>1</sup> R.J. Jensen, Fusion Technology **11**, 481 (1987).
- <sup>2</sup> M.W. McGeoch, P.A. Corcoran, R.G. Altes, I.D. Smith, S.E. Bodner, R.H. Lehmberg, S.P. Obenschain, and J.D. Sethian, Fusion Technology **32**, 610 (1997).
- <sup>3</sup> J.D. Sethian, C.J. Pawley, S.P. Obenschain, K.A. Gerber, V. Serlin, C.A. Sullivan, T. Lehecka, W.D. Webster, M.W. McGeoch, I.D. Smith, P.A. Corcoran, and R.A. Altes, IEEE Trans. Plasma Sci. **25**, 221 (1997).
- <sup>4</sup> J.D. Sethian, S.P. Obenschain, K.A. Gerber, C.J. Pawley, V. Serlin, C.A. Sullivan, W.D. Webster, A.V. Deniz, T. Lehecka, M.W. McGeoch, R.A. Altes, P.A. Corcoran, I.D. Smith, and O.C. Barr, Rev. Sci. Instrum. **68**, 2357 (1997).
- <sup>5</sup> J.D. Sethian, M. Meyers, I.D. Smith, V. Carboni, J. Kishi, D. Morton, J. Pearce, B. Bowen, L. Schlitt, O. Barr, and W. Webster, IEEE Trans. Plasma Sci. **28**, 1333 (2000).
- <sup>6</sup> I. Okuda, J. Ma, E. Takahashi, I. Matsushima, Y. Matsumoto, S. Kato, Y. Owadano, Appl. Phys. B **72**, 623 (2001).
- <sup>7</sup> I. Okuda, E. Takahashi, I. Matsushima, Y. Matsumoto, S. Kato, Y. Owadano, Jpn. J. Appl. Phys. **40**, 1152 (2001).
- <sup>8</sup> G.M. Petrov, J.L. Giuliani, and A. Dasgupta, "Electron energy deposition in an e-beam pumped KrF amplifier: impact of the beam power and energy", J. Appl. Phys., **91**, 2662 (2002).
- <sup>9</sup> L.R. Peterson and J.E. Allen, J. Chem. Phys. **56**, 6068 (1972).
- <sup>10</sup> T.H. Johnson and A.M. Hunter, J. Appl. Phys. **51**, 2406 (1980).
- <sup>11</sup> W.L. Morgan and A. Szöke, Phys. Rev. A **23**, 1256 (1981).
- <sup>12</sup> A. Mandl, D. Klimek, and J.H. Parks, J. Appl. Phys. **55**, 3940 (1984).

- <sup>13</sup> F. Kannari, M. Obara, and T. Fujioka, J. Appl. Phys. **57**, 4309 (1985).
- <sup>14</sup> S.J. Czuchlewski, D.E. Hanson, B.J. Krohn, and A.R. Larson, Fusion Technology **11**, 560 (1987).
- <sup>15</sup> W.L. Nighan, Appl. Phys. Lett., **32**, 297 (1978).
- <sup>16</sup> A. Suda, H. Kumagai, and M. Obara, Appl. Phys. Lett. **51**, 218 (1987).
- <sup>17</sup> W.L. Morgan, Plasma Chem. Plasma Process. **12**, 449 (1992).
- <sup>18</sup> D.L. McCorkle, L.G. Christophorou, A.A. Christodoulides, and L. Pichiarella, J. Chem. Phys. **85**, 1966 (1986).
- <sup>19</sup> M.J. Kushner and T.J. Moratz, Appl. Phys. Lett. **52**, 1856 (1988).
- <sup>20</sup> M. Hayashi and T. Nimura, J. Appl. Phys. **54**, 4879 (1983).
- <sup>21</sup> M. Elyaakoubi and P. Ranson, J. Appl. Phys. **78**, 4733 (1995).
- <sup>22</sup> L.G. Christophorou, *Atomic and Molecular Radiation Physics* (Wiley-Interscience, London, 1971), p.35.

## TABLES

TABLE I. Rate coefficients for attachment, vibrational excitation, and dissociation.  $x_{F_2}$  is the number mole fraction of  $F_2$ .  $P_{beam}$  is the electron beam power density in units of MW/cm<sup>3</sup>.

process	k ( $10^{-10}$ cm <sup>3</sup> s <sup>-1</sup> )
attachment $k^{att}$	$3.6 x_{F_2}^{-0.3} P_{beam}^{+0.12}$
vibrational excitation $k^{vib}$	$(18+12e^{-100x_{F_2}})P_{beam}^{+0.06}$
direct dissociation $k^{dis}$	$(2.8+19x_{F_2}^{0.3})P_{beam}^{-0.06}$

## FIGURES

FIG. 1. EEDF for fluorine mole fraction varying from 0.1% to 3% for  $p_{Ar}=562.5$  Torr,  $p_{Kr}=254.4$  Torr,  $P_{beam}=346$  kW/cm<sup>3</sup> and  $U_{beam}=100$  keV. (a) The distribution function in density units and (b) normalized to unity.

FIG. 2. Electron density and mean energy versus fluorine mole fraction. The rare gas pressures and beam parameters are the same as in Fig. 1.

FIG. 3. Rate coefficients for various processes in Ar (a), Kr (b), and F<sub>2</sub> (c) versus fluorine mole fraction. The rare gas pressures and beam parameters are the same as in Fig. 1.

FIG. 4. Fractional power loss in electron collisions with Ar (a), Kr (b), and F<sub>2</sub> (c) versus fluorine mole fraction. The rare gas pressures and beam parameters are the same as in Fig. 1.

FIG. 5. EEDF for Kr mole fraction of 10%, 50% and 90% for  $p_{Ar} + p_{Kr} + p_{F_2}=820.8$  Torr,  $p_{F_2}=3.9$  Torr,  $P_{beam}=346$  kW/cm<sup>3</sup> and  $U_{beam}=100$  keV.

FIG. 6. Rate coefficients for Ar (a), Kr (b) and F<sub>2</sub> (c) versus Kr mole fraction. The gas pressures and beam parameters are the same as in Fig. 5.

FIG. 7. Fractional power loss in electron collisions with Ar (a), Kr (b) and F<sub>2</sub> (c) versus Kr mole fraction. The gas pressures and beam parameters are the same as in Fig. 5.

FIG. 8. Total excitation to ionization ratio for Ar, Kr and F<sub>2</sub> versus Kr mole fraction at different fluorine mole fractions. The beam power and energy are  $P_{beam}=346$  kW/cm<sup>3</sup> and  $U_{beam}=100$  keV.

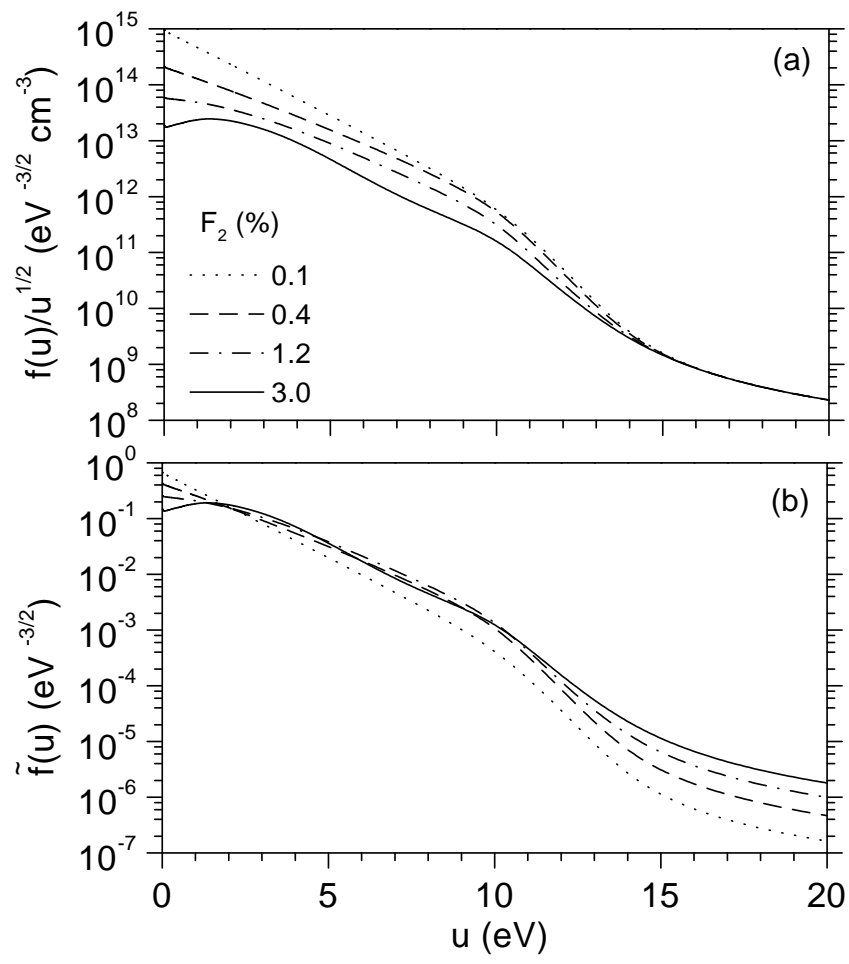


Fig.1

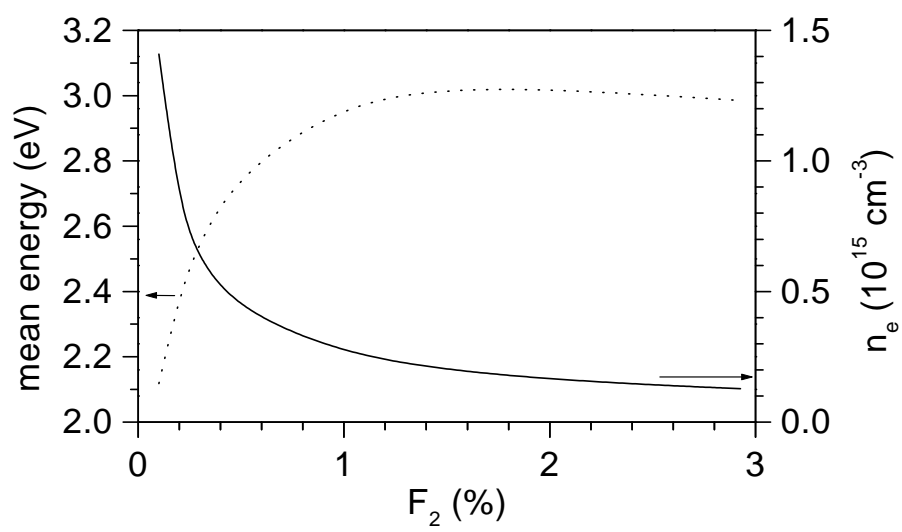


Fig.2

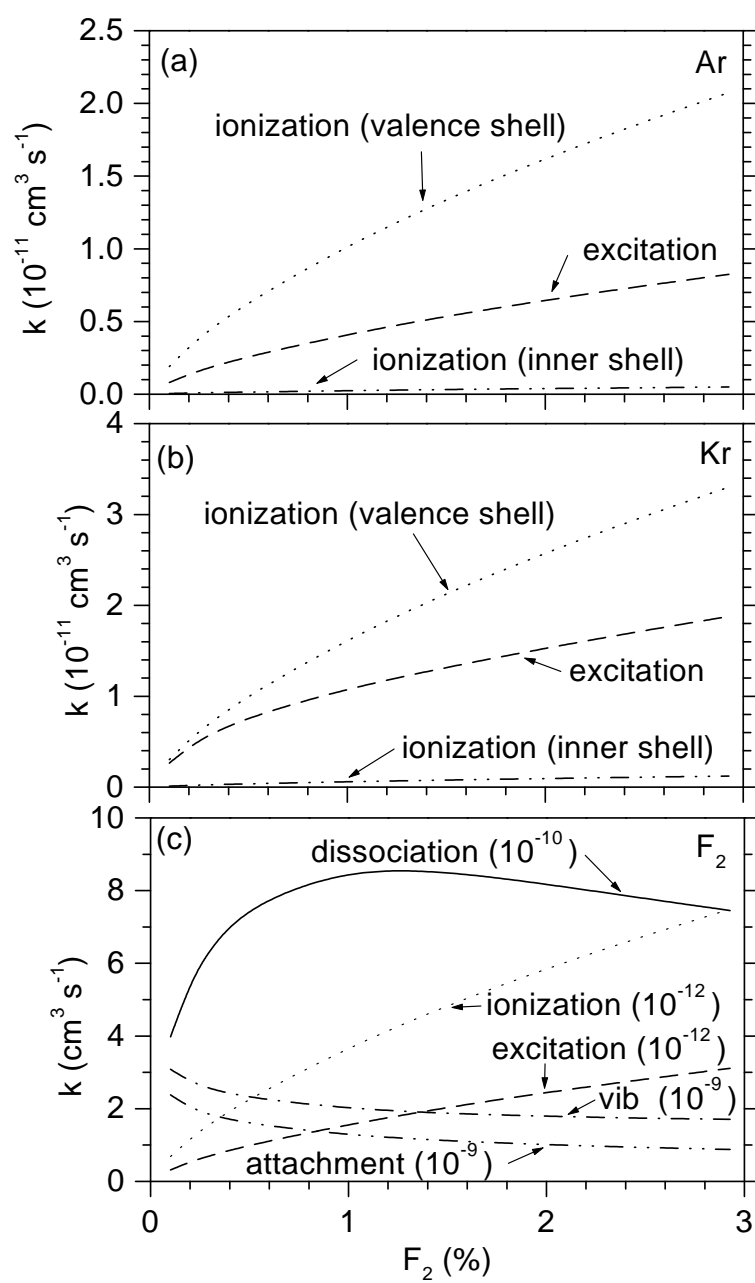


Fig.3

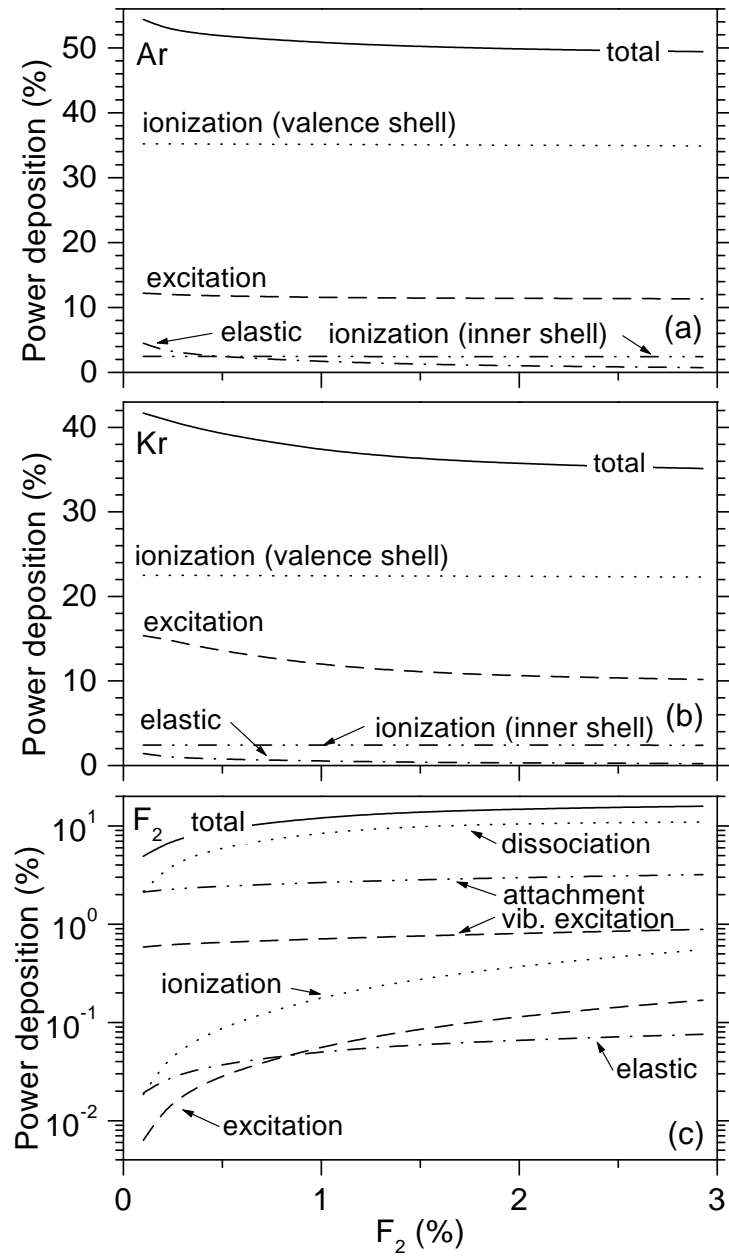


Fig.4

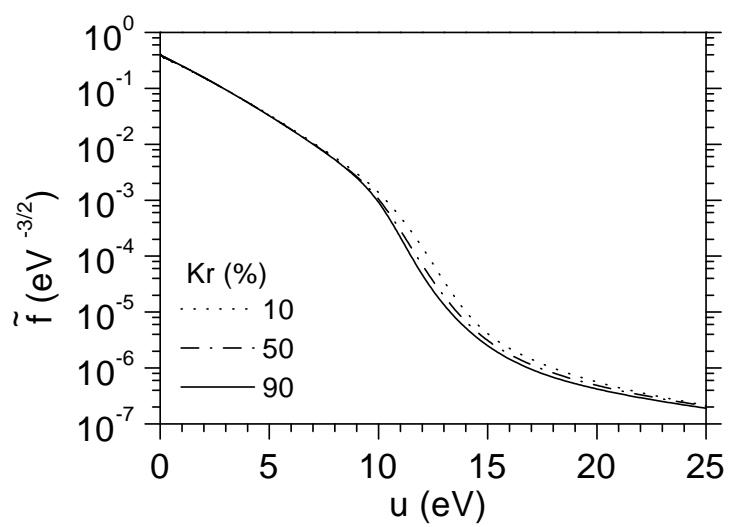


Fig.5

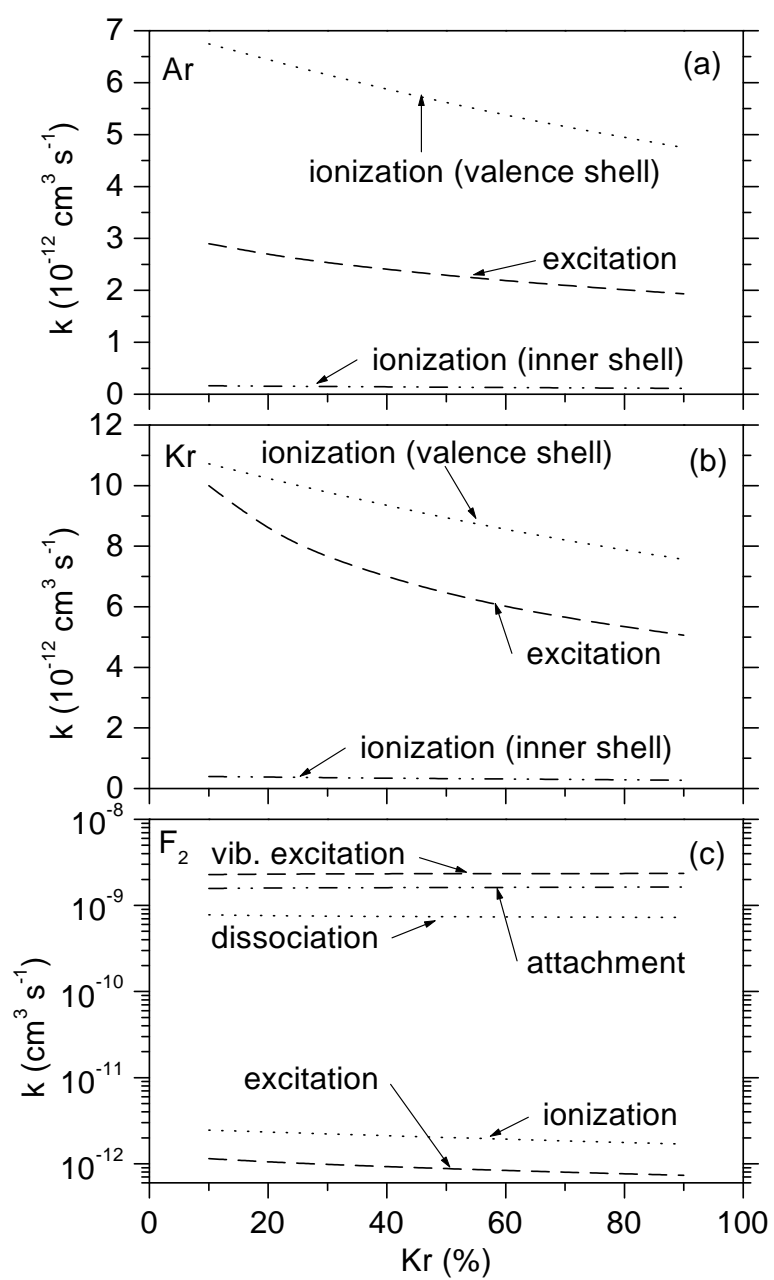


Fig.6

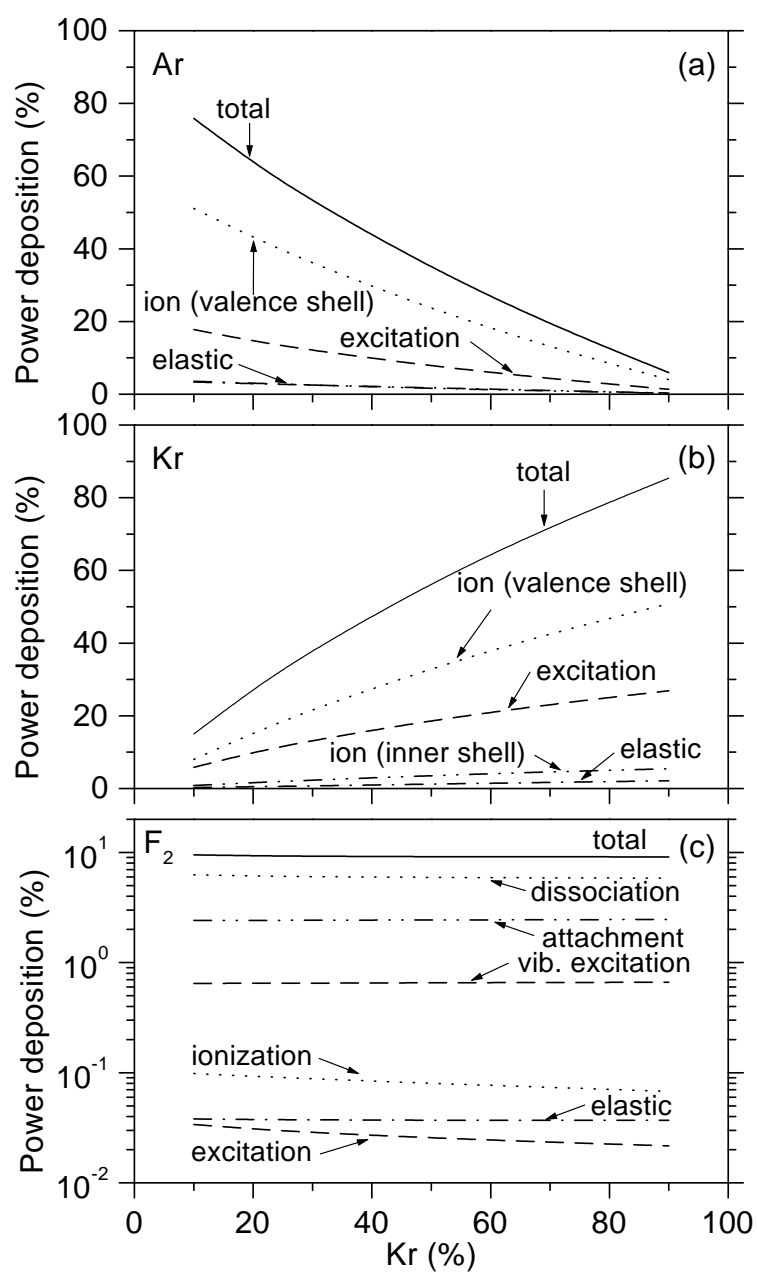


Fig.7

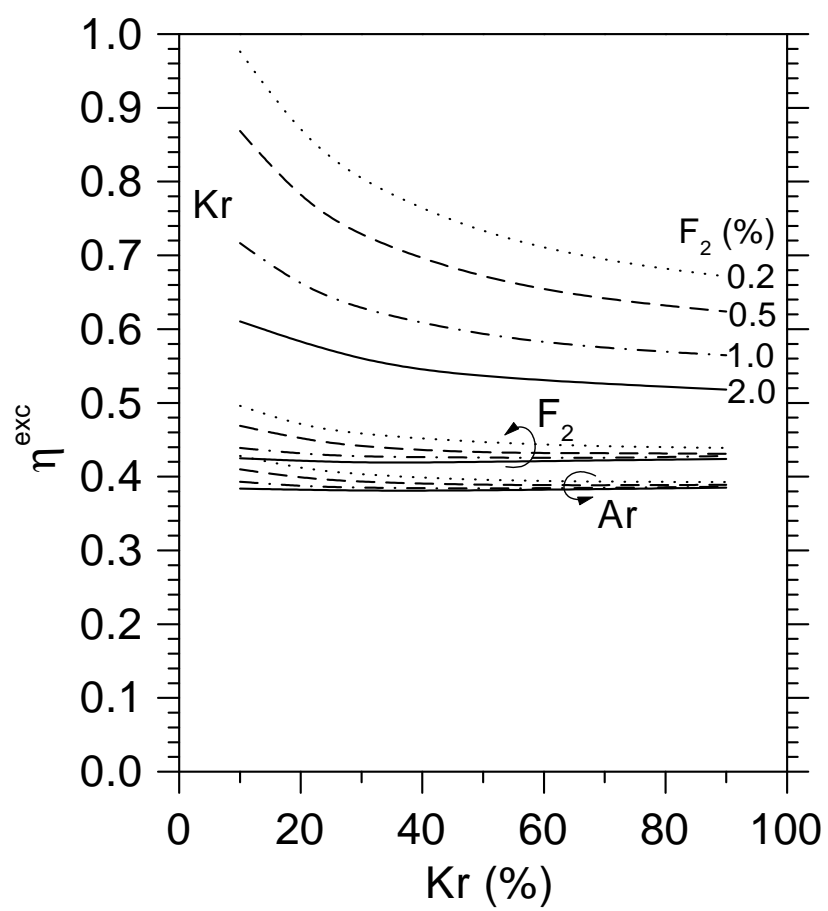


Fig.8